UR1984_04 1/27

The petrology, mineralogy and geochemistry of the Pyengana and Gardens granodiorites, the Hogans Road diorite and the dolerite dykes of the Blue Tier Batholith.

M.P. McClenaghan

Abstract

The petrology and mineralogy of the Gardens and Pyengana grandoriorites, the Hogans Road diorite and the dolerite dykes of the Blue Tier Batholith is described. Geochemical data on these bodies are presented and their petrogenesis is discussed. It is suggested that there is a genetic link between these rock bodies.

INTRODUCTION

The Blue Tier Batholith in north-eastern Tasmania is a composite, essentially post-kinematic, granitoid mass intruded at high level. Biotite igneous ages and Sr/Rb isochron ages range from 395 to 370 Ma (Cocker, 1982). Plutons extend in composition from granodiorite to alkali-feldspar granite. The batholith is part of the south-east Australian tin province and since the genesis of tin is linked to genesis of the batholith as a whole, it has attracted considerable attention and a number of petrogenetic models have been put forward. McCarthy and Groves (1979) suggested that the geochemical variation between plutons can be explained by the progressive accumulation of crystals from a fractionally crystallising adamellitic melt. Cocker (1977) proposed that individual plutons result from crystallisation of melts derived from discrete source rocks of differing chemical composition without any inter-pluton fractionation. McClenaghan and Williams (1982) suggested a connection between adamellite and alkali-feldspar granite plutons by crystal fractionation or by a combination of restite unmixing and crystal fractionation. Higgins *et al.* (1983) also suggested that alkali-feldspar granite could be derived from the adjacent adamellites by fractional crystallisation. They further concluded that, within a pluton, variation could be explained by fractional crystallisation but that the adamellites and alkali-feldspar granites could not be derived from the granodiorites by fractional crystallisation. The lack of connection between the granodiorites and the other rock types in the batholith seems particularly convincing. A three-fold division of the rocks of the batholith into granodiorite, adamellite and alkali granite (now-termed alkali-feldspar granite) suites was proposed by McClenagahn *et al.* (1982) on the basis of distinctly different trends for major and trace elements on Harker variation diagrams. The lower initial $^{87}Sr/^{86}Sr$ ratios for the granodiorites (0.7061 - 0.7073) than for the adamellites (0.7070 - 0.7105, Cocker, 1982) supports this division, as does the difference in rare earth patterns (Higgins *et al.*, 1983). Based on mineralogy and chemical composition Cocker (1977) and McClenaghan *et al.* (1982) concluded that the granodiorites had I-type characteristics while the adamellites were S-type (White and Chappell, 1977).

This paper presents new data on the Gardens and Pyengana granodiorites, the Hogans Road diorite and a dolerite dyke suite present throughout most of the batholith. The Hogans Road diorite is the most basic rock so far described in the batholith, and if it can be shown to be involved in its evolution, it may have an important bearing on any petrogenetic model. The dolerite dykes occur widely in the granitoid areas and have been reported to occur as far north as the Furneaux Group and as far south as Coles Bay (Cocker, 1977). The dykes intrude all granite types; however, near Lady Barron on Flinders Island a dolerite dyke is intruded by a quartz-feldspar porphyry dyke (pers. comm. P.W. Baillie and N.J. Turner). Since the

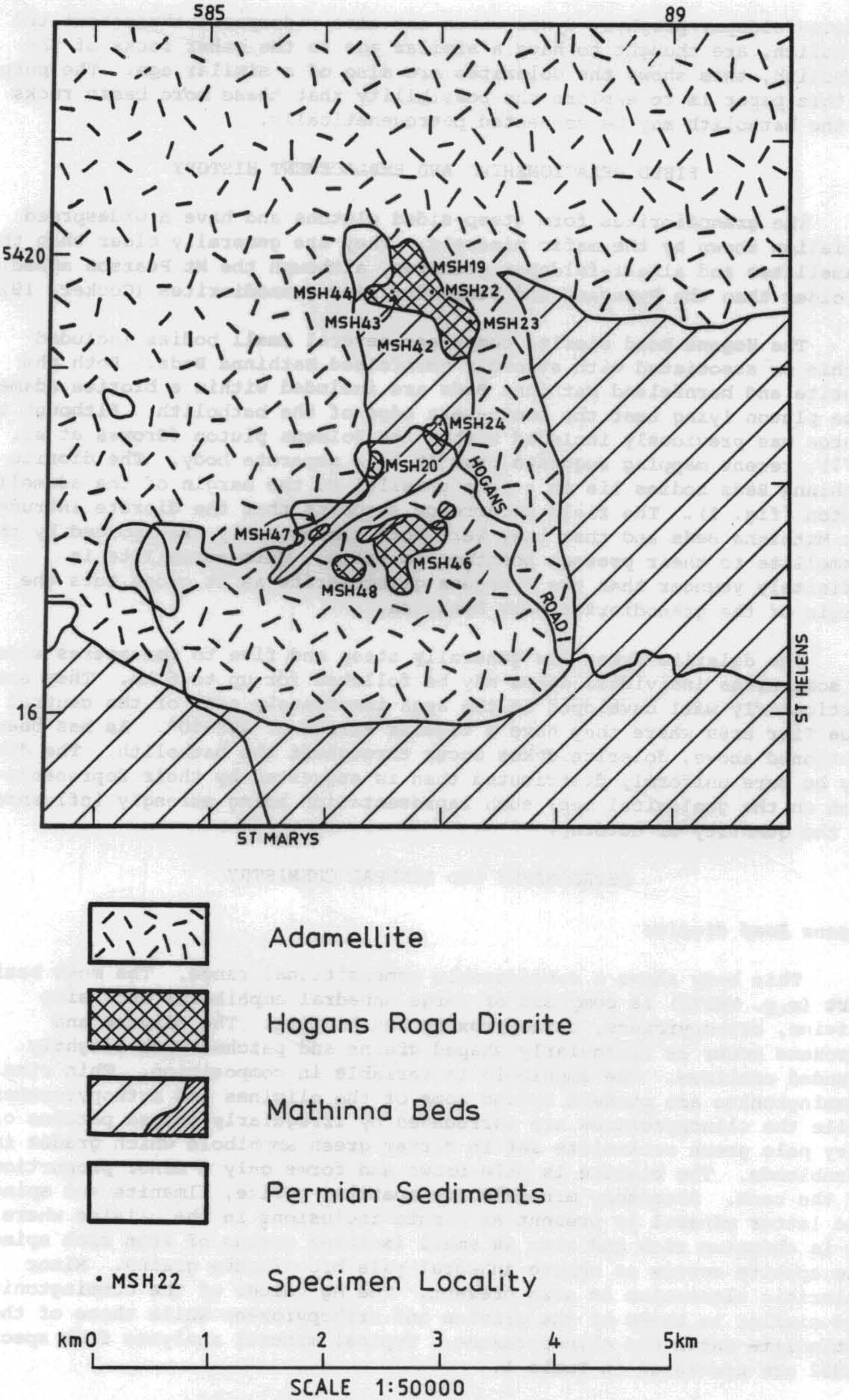

Figure 1. *Geological map showing the distribution of the Hogans Road diorite.*

quartz-feldspar porphyry dykes which are also widespread throughout the batholith, are thought to have a similar age to the other rocks of the batholith, this shows the dolerites are also of a similar age. The purpose of this paper is to explore the possibility that these more basic rocks of the batholith may be connected petrogenetically.

FIELD RELATIONSHIPS AND EMPLACEMENT HISTORY

The granodiorites form steep-sided plutons and have a widespread foliation shown by the mafic minerals. They are generally older than the adamellites and alkali-feldspar granites, although the Mt Pearson adamellite is older than the Pyengana and Scamander Tier granodiorites (Cocker, 1977).

The Hogans Road diorite comprises several small bodies included within or associated with strongly hornfelsed Mathinna Beds. Both the diorite and hornfelsed Mathinna Beds are included within a biotite adamellite pluton lying near the south-west edge of the batholith. Although this pluton was previously included within the Poimena pluton (Groves *et al.* 1977), recent mapping suggests that it is a separate body. The diorite and Mathinna Beds bodies lie in a zone parallel to the margin of the adamellite pluton (fig. 1). The field occurrence suggests that the diorite intruded the Mathinna Beds and that they were both subsequently transported by the adamellite to their present position as rafts. This adamellite is definitely younger than the Pyengana granodiorite as it cross cuts the margin of the granodiorite near Pyengana.

The dolerite dykes are generally steep and five to ten metres wide. In some areas individual dykes may be followed for up to 6 km. They are particularly well developed in the area immediately east of the central Blue Tier area where they have a regular strike of 40°-50°. As has been mentioned above, dolerite dykes occur throughout the batholith. The dykes may be more uniformly distributed than is suggested by their representation on the geological map; such representation being strongly influenced by the quantity of outcrop.

PETROGRAPHY AND MINERAL CHEMISTRY

Hogans Road diorite

This body shows a considerable compositional range. The most basic part (*e.g.* MSH22) is composed of large anhedral amphiboles enclosing olivine, orthopyroxene, clinopyroxene and biotite. The olivine and pyroxene occur as irregularly shaped grains and patches with slightly rounded outlines. The amphibole is variable in composition. Thin rims of cummingtonite are present around some of the olivines and orthopyroxenes while the clinopyroxenes are surrounded by irregularly shaped patches of very pale green actinolite set in darker green amphibole which grades into hornblende. The biotite is pale brown and forms only a minor proportion of the rock. Accessory minerals are apatite, pyrite, ilmenite and spinel. The latter mineral is present as minute inclusions in the olivine where it is chromium rich and also as small isolated grains of iron rich spinel. The apatite occurs as sparse anhedral pale brown/mauve grains. Minor chloritic alteration is also present. The Mg values of the cummingtonite are similar to those of the olivine and orthopyroxene while those of the actinolite match the clinopyroxene. Typical mineral analyses from specimen MSH22 are presented in Table 1.

In less basic parts of the body the rock contains plagioclase and quartz but olivine and orthopyroxene are absent. Amphibole is still present as large anhedral crystals and has inclusions of anhedral grains of clinopyroxene, plagioclase and biotite. Quartz is intergranular and the biotite is more abundant and darker brown. Amphibole has a range of composition from actinolite to hornblende. Plagioclase contains sericitically altered cores with sharp boundaries with clear slightly zoned rims. There is a gap in compositional ranges between the cores (An 76.6-92.8) and the rims (An 42.0-50.5). Accessory minerals are apatite, pyrite, ilmenite zircon and prehnite. The latter mineral occurs as thin strips along the cleavage in biotites.

In the least basic part of the body the amphiboles are smaller and the clinopyroxene is absent but otherwise the rock is very similar to that described above. Typical mineral analyses from the less basic parts of the body are presented in Table 2.

Gardens and Pyengana granodiorites

The Gardens granodiorite consists of euhedral to anhedral amphibole and biotite, plagioclase and intergranular K-feldspar and quartz. The amphibole ranges in composition from actinolite to hornblende with core regions of crystals being actinolite while marginal zones and the euhedral crystals are hornblende. Among the more basic specimens (*e.g.* BT3/58, MBT258) clinopyroxene is present as small anhedral grains and patches associated with the actinolite. The biotite and amphibole occur intermingled in patches as well as in isolated crystals and the amphibole contains inclusions of biotite and small quartz grains. The plagioclase frequently contains sericitically altered core regions that have sharp boundaries with clear rim zones. The core regions have a compositional range of An 81.2-68.6 which does not overlap with that of the rims (An 52.4-38.5). Accessory minerals are apatite, sphene, ilmenite and zircon. Prehnite is developed as thin strips along the cleavage of the biotites. Minor chloritic alteration of the biotite is also present. Representative mineral compositions are presented in Table 3.

The Pyengana granodiorites are generally very similar but have not been found to contain clinopyroxene. The amphibole is darker green and actinolite is less abundant. The plagioclase shows sericitic alteration of the central areas; however, a sharp boundary between the core and rim regions is not present and the cores are less calcic (An <58.5) than for the Gardens rocks. Accessory minerals are apatite, magnetite, zircon and allanite. The magnetite occurs as isolated grains and also as clusters of grains associated with the hornblende and biotite. Chloritic alteration of the biotites is more extensive than for the Gardens granodiorite. Prehnite is developed along the biotite cleavages. Representative mineral compositions are presented in Table 4.

Dolerite dykes

The dolerite dykes consist of a framework of plagioclase laths with intergranular and sub-ophitic clinopyroxene and abundant grains of ilmenite. Accessory minerals are apatite, sphene and pyrite. In some specimens there is minor alteration of the clinopyroxene to amphibole together with chlorite, while in other specimens the clinopyroxene is completely replaced by green hornblende and a small quantity of biotite is also present. Orthopyroxene is rarely present. Representative mineral analyses are presented in Tables 5, 6.

5 cm

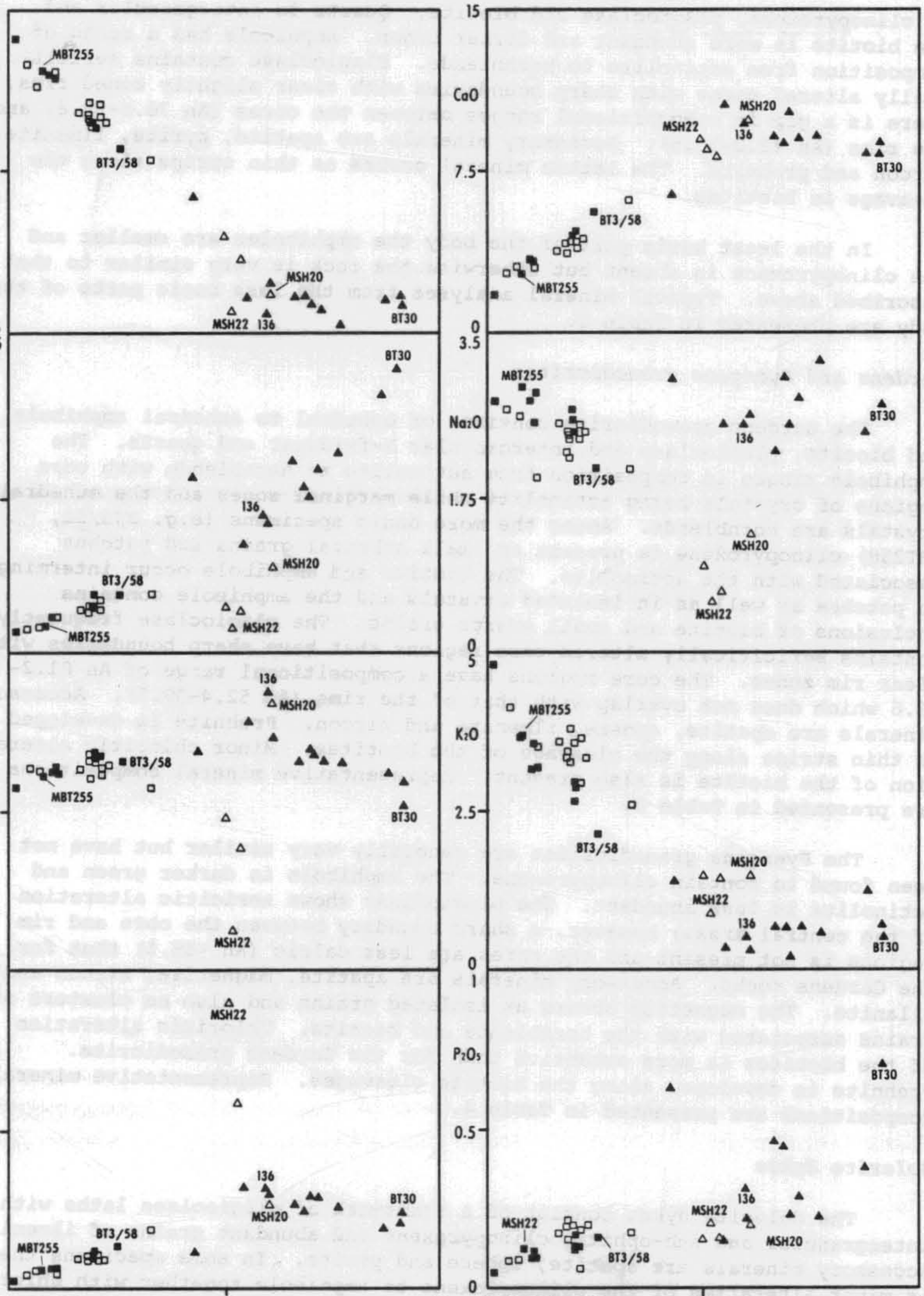

Figure 2. *FeO total, SiO_2, TiO_2, Al_2O_3, MgO, CaO, Na_2O, P_2O_5 and K_2O variation in the granodiorites, diorites and dolerite dykes of the Blue Tier Batholith. Symbols:* □ *Pyengana pluton,* ■ *Gardens Pluton,* △ *Hogans Road diorite,* ▲ *dolerite dykes. Some of the specimens used in the mixing calculations are labelled. Trend line arrows indicate direction of increasing $Fe^{+2}total/Fe^{+2}total + Mg$.*

5 cm

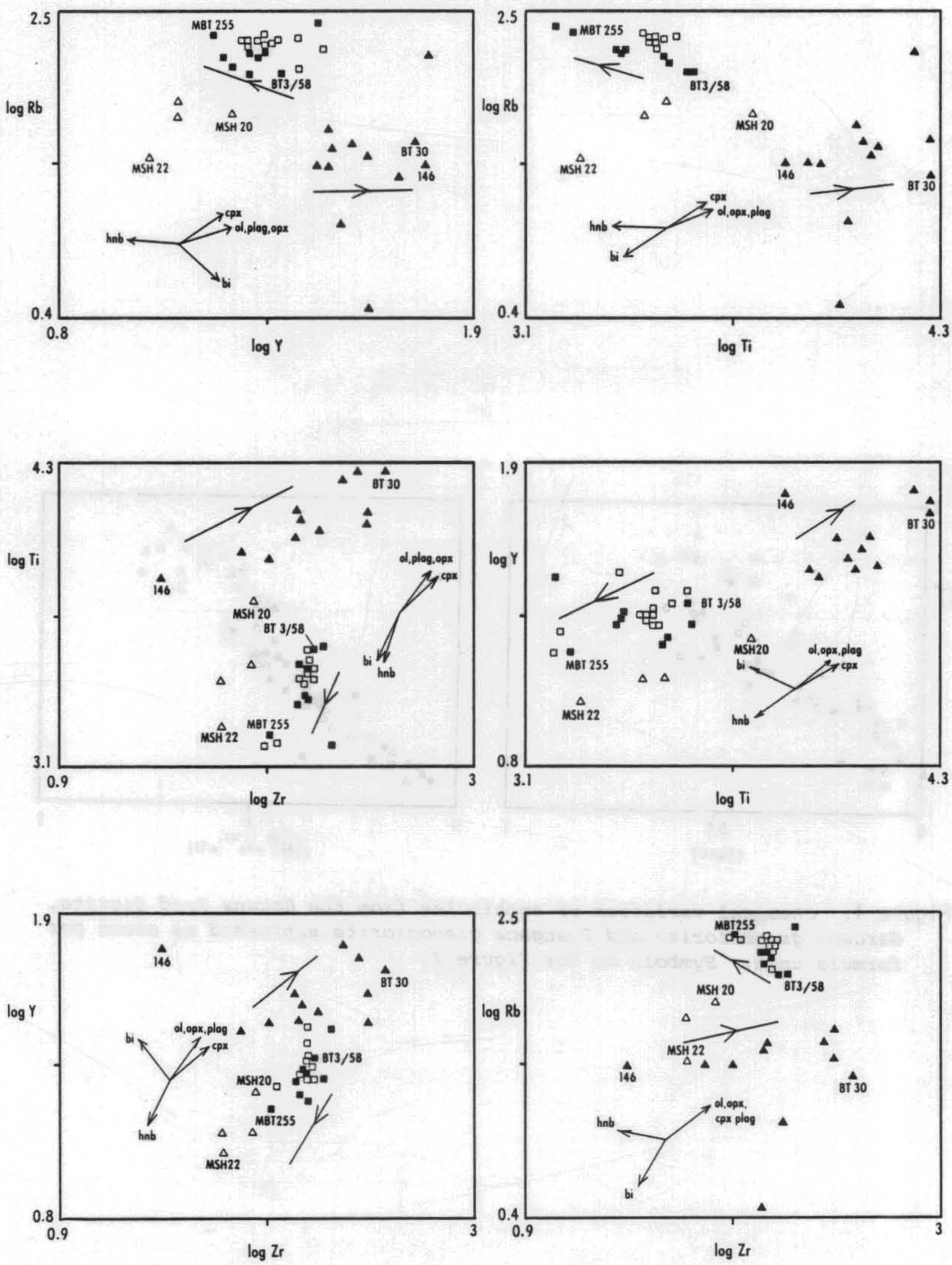

Figure 3. *Ti, Zr, Rb and Y variation in the granodiorites, diorites and dolerite dykes of the Blue Tier Batholith. Symbols and labels as for Figure 2.*

5 cm

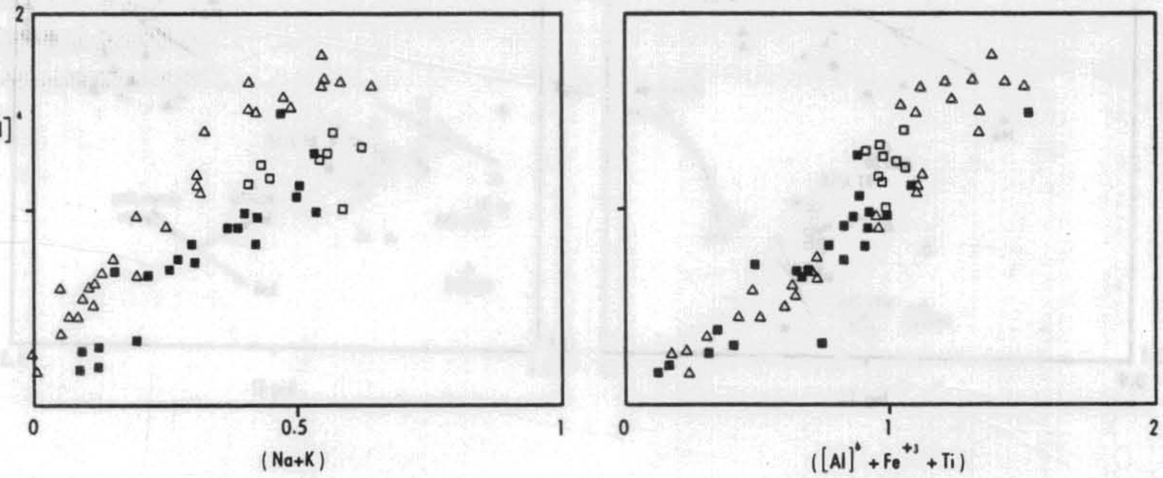

Figure 4. *Chemical variation of amphiboles from the Hogans Road diorite, Gardens granodiorite and Pyengana granodiorite expressed as atoms per formula unit. Symbols as for Figure 2.*

GEOCHEMISTRY AND GEOCHEMICAL MODELLING

Introduction

In Appendix 1 seventeen new whole rock analyses of the Gardens and Pyengana plutons together with four analyses of the Hogans Road diorite are presented. In Appendix 2 seven new analyses of dolerites from the area covered by the Blue Tier map sheet are presented together with five analyses reproduced from McClenaghan *et al.* (1982). Six analyses of the Pyengana pluton listed in Higgins *et al.*, 1983 are used in plotting the variation diagrams (fig. 2, 3).

Hogans Road diorite

The very high MgO content (22.58 mass%) of the most basic of Hogans Road diorites (MSH22) suggests that it is an accumulate rock. The present texture of large poikilitic amphiboles forming the bulk of the rock is metamorphic or metasomatic, however, the anhedral and slightly rounded grains of olivine, orthopyroxene and clinopyroxene may represent the remnants of an original accumulate mineralogy. The olivine cannot have crystallised from a melt of the composition of the host rock based on a distribution coefficient ($K_{D(Fe-Mg)}^{ol/l}$) of 0.3 Roeder (1974). Table 7 shows distribution coefficients calculated for the analysed rocks from the Hogans Road diorite and an olivine from MSH22. The olivine could have crystallised from a melt of the composition of MSH20 but not from any of the other rocks. This suggests that MSH20 and MSH22, which lie on each extreme of the composition range shown by the Hogans Road diorite, may be connected by varying amounts of mineral accumulation. A mixing calculation (Le Maitre, 1979) involving these two compositions gives a moderately good fit (table 8A). It is probable that the original composition of these rocks may have been changed by metasomatism during the time they were suspended as rafts in the host adamellite and so explain why the fit is not more exact. Another mixing calculation (table 8B) shows that MSH22 approximates closely to an olivine, orthopyroxene, clinopyroxene and plagioclase rock with the addition of a small amount of water and potash.

The plot positions of the four Hogans Road diorite samples on the variation diagrams (fig. 2, 3) is consistent with the accumulation model suggested above. The single mineral fractionation vectors drawn on the trace element variation diagrams show that those for olivine, orthopyroxene and clinopyroxene are close to parallel to a trend defined by the most and least basic diorites (MSH22 and MSH20).

Gardens and Pyengana granodiorites

The Gardens and Pyengana granodiorites define trends on the major and trace element variation diagrams (fig. 2, 3). The trends are almost the same for most elements the exceptions being Na_2O, K_2O and Rb. The Gardens pluton is less potassic and more sodic than the Pyengana pluton. These differences suggest a slightly different evolutionary history.

The trends on the trace element diagrams are consistent with fractionation dominated by hornblende and to a lesser extent plagioclase. A mixing calculation for the Pyengana pluton using two compositions from the extremes of the trend shows that a good fit can be obtained by fractionation of hornblende, plagioclase, biotite and minor amounts of apatite and sphene (table 5C). A similar calculation for the Gardens pluton shows that a slightly less good fit can be obtained with the same minerals except that a small quantity of ilmenite replaces the sphene and apatite. The quantity of biotite is much less and hornblende is a larger component. The first of these calculations is similar to that presented by Higgins *et al.* (1983) for the Pyengana pluton. This model of hornblende and plagioclase dominated fractionation is in agreement with the petrography of the granodiorites since these minerals clearly crystallised before the quartz and K-feldspar and were thus available as fractionating phases.

Dolerite dykes

The dolerite dykes define a trend on the variation diagrams (fig. 2, 3). The direction of evolution is towards decreasing Mg/Mg + Fe^{+2} total values. The largest compositional changes along the trend for major elements are increasing total iron and TiO_2 with falls in CaO, MgO and Al_2O_3. Among the trace elements the greatest variation is in Zr which shows a large increase. The trends on the trace element variation diagrams (fig. 3) are approximately parallel to the fractionation vectors for olivine, orthopyroxene, clinopyroxene and plagioclase except for the diagrams involving Rb. It is possible there may have been Rb contamination from the host rock granite which would explain this discrepancy. The trends for the least mobile elements Zr, Ti and Y are consistent with fractionation of the minerals listed above. If a fractionation process did operate then it is clear that a very large amount of fractionation would have had to have taken place in order to produce the large increase in TiO_2 and particularly Zr. Using the Rayleight equation ($C^1/C^0=F^{(D-1)}$) and assuming a D value of 0 and using the Zr of the rocks at the extremes of the trend (C^1 = 363 specimen BT30, C^0 = 26 specimen 146) it can be calculated that F, the weight proportion of residual liquid, would be 0.072. This would be the minimum amount of fractionation since D must be greater than 0. The bulk composition of the fractionating minerals would have had to have been close to the composition of the host magma. This would have been consistent with fractionation of a combination of the minerals listed above.

Relationship between the Hogans Road diorite, the granodiorites and the dolerite dykes

A number of common petrographic features link the Hogans Road diorite with the granodiorites, particularly with the Gardens granodiorite. These are as follows: plagioclases with anorthite rich cores having a distinct gap in compositional ranges with the rims (tables 2, 3), clinopyroxene inclusions in the amphiboles, an overlapping range of amphibole composition from actinolite to hornblende (fig. 4). The least basic diorite sample plots close to the extrapolation of the granodiorite trends on the major element variation diagrams (fig. 2). On the trace element variation diagrams (fig. 3) it is clear that this sample is too low in Ti, Y, Rb and Zr to be a sample of a magma directly parental to the granodiorites, however, the fractionation vectors for olivine, orthopyroxene, clinopyroxene and plagioclase indicate that fractionation of these minerals from the least basic diorite would drive a residual liquid towards a composition that would lie on the extrapolation of the granodiorite trends. Alternatively accumulation of these minderals in a magma parental to the granodiorites could have produced the diorites. Since these minerals are present in the diorite either seems possible.

The extrapolation of the granodiorite trends intersects the dolerite trend for all the major elements and trace elements on the variation diagrams (figs. 2, 3) except for Na_2O. Since these trends have been postulated to have been caused by fractionation dominated by hornblende and plagioclase a mixing calculation has been made to see if fractionation of the same minerals from one of the dolerites could produce the most basic granodiorite on the Gardens trend. This calculation shows that a fairly good fit can be obtained if the fractionation minerals were hornblende, plagioclase, biotite and small amounts of ilmenite and apatite (Tabe 8E). Most of the discrepancy is accounted for by Na_2O. It is possible that this may be explained by Na_2O mobility. The calculation also shows that a very large amount of fractionation would be required. If a magma of the dolerite composition was parental to the granodiorites then it must have been of approximately forty times greater volume than the granodiorites. The lack of gravity evidence for a large basic body in the upper crust (Leaman and Symonds, 1975) indicates it would have to be located at considerable depth, probably near the base of the crust. Also if such a vast body of basic magma were in the upper crust the heating effect would have produced considerable metamorphism in the rocks now at the surface. Slow cooling of such a body with crystallisation and separation of anhydrous minerals such as olivine, pyroxene and plagioclase would raise the water content and reduce the viscosity and density of the residual liquid until a body of residual magma was forced to rise through the crust because of its lower density compared to that of the surrounding rocks. The greater water content would have caused the mafic minerals to react to form hornblende and biotite. Fractionation of these minerals together with plagioclase would eventually have produced the granodiorites. The considerable heating effect of the large basic magma body at depth might be expected to have produced localised melting in the lower crust and this may have been the source of the adamellites which appear to have been derived from the melting of sedimentary rocks. In this model the dolerite dykes which appear to be later than most of the granitoid activity, would have been produced by direct tapping of the remnants of the large basic magma body. The dykes would have issued from different parts of the basic body which had undergone different degrees of fractionation and increase in water content thus explaining their compositional variation and state of hydration.

The model explains the lack of chemical and isotopic continuity between the granodiorites and the more acidic bodies in the batholith since it postulates they formed from different magmas derived from different source rocks. Since, however, the granodiorites occur in the same area and were intruded at nearly the same time as the more acidic rocks a link would be expected between them. This link is the heating effect of the basic parental magma to the granodiorites which caused melting in the crust of sedimentary rocks which in turn gave rise to the adamellites. It seems possible that the parental basic magma might issue a number of diapirs giving granodiorites over a period of time, some of which would be later than some of the adamellite bodies. The model may be tested by Sr isotope and rare earth measurements on the Hogans Road diorite and the dolerite dykes.

It is quite possible that the link between the dolerite dykes and the granodiorites suggested above is not real and that the granodiorites were produced by melting of some igneous rock deep in the crust under the influence of heat introduced by the basic magma parental to the dolerite dykes.

CONCLUSION

Attention has been drawn to rocks in the batholith more basic than the granodiorites and a model linking them has been suggested. It is clear that the model is highly speculative and more work will be required to test it.

REFERENCES

COCKER, J.D. 1977. *Petrogenesis of the Tasmanian granitoids*. Ph.D. thesis, University of Tasmania : Hobart.

COCKER, J.D. 1982. Rb-Sr geochronology and Sr isotopic composition of Devonian granitoids, eastern Tasmania. *J.geol.Soc.Aust.* 29:139-158.

GROVES, D.I.; COCKER, J.D.; JENNINGS, D.J. 1977. The Blue Tier Batholith. *Bull.geol.Surv.Tasm.* 55.

HIGGINS, N.C.; SOLOMON, M.; VARNE, R. 1983. The genesis of the granitoids of the Blue Tier Batholith, N.E. Tasmania. *Geochim.cosmochim.Acta.* (in press).

LEAMAN, D.E.; SYMONDS, P.A. 1975. Gravity survey of north-eastern Tasmania. *Pap.geol.Surv.Tasm.* 2.

Le MAITRE, R.W. 1979. A new generalised petrological mixing model. *Contrib.Mineral.Petrology* 71:133-137.

McCARTHY, T.S.; GROVES, D.I. 1979. The Blue Tier Batholith, north-eastern Tasmania. A cumulate-like product of fractional crystallisation. *Contrib.Mineral.Petrology* 71:193-209.

McCLENAGHAN, M.P.; TURNER, N.J.; BAILLIE, P.W.; BROWN, A.V.; WILLIAMS, P.R.; MOORE, W.R. 1982. Geology of the Ringarooma-Boobyalla area. *Bull. geol.Surv.Tasm.* 61.

McCLENAGHAN, M.P.; WILLIAMS, P.R. 1982. Distribution and characterisation of granitoid intrusions in the Blue Tier area. *Pap.geol.Surv.Tasm.* 4.

PAPIKE, J.J.; CAMERON, K.L.; BALDWIN, K. 1974. Amphiboles and pyroxenes : characterization of other than quadrilateral components and estimates of ferric iron from microprobe data. *Abstr.Prog.geol.Soc.Am.* 6:1053-1054.

PERFIT, M.R.; BRUECKNER, H.; LAWRENCE, J.R.; KAY, R.W. 1980. Trace element and isotopic variations in a zoned pluton and associated volcanic rocks, Unalaska island, Alaska : A model for fractionation in the Aleutian calcalkaline suite. *Contrib.Mineral.Petrology* 73:69-87.

PEARCE, J.A.; NORRY, M.J. 1979. Petrogenetic implications of Ti, Zr, Y and Nb variations in volcanic rocks. *Contrib.Mineral.Petrology* 69:33-47.

ROEDER, P.L. 1974. Activity of iron and olivine solubility in basaltic liquids. *Earth.planet.Sci.Lett.* 23:397-410.

WHITE, A.J.R.; CHAPPELL, B.W. 1977. Ultrametamorphism and granitoid genesis. *Tectono-physics* 43:7-22.

[13 January 1984]

Table 1. REPRESENTATIVE ANALYSES FROM THE MOST MAFIC HOGANS ROAD DIORITE MSH22.

Analysis No.	1 Olivine		2 Orthopyroxene	3 Clinopyroxene		4 Cummingtonite
SiO_2	39.25		56.01	53.38		57.74
TiO_2	0		0	0		0
Al_2O_3	0		1.08	0.77		0.81
Cr_2O_3	0		0	0.51		0
Fe_2O_3	0		0.33	0		0
FeO	16.65		10.64	2.98		11.70
MnO	0.18		0.18	0		0.37
MgO	43.90		30.90	17.15		26.08
CaO	0		0.84	24.19		1.12
Na_2O	0		0	0		0
K_2O	0		0	0		0
H_2O	0		0	0		2.18
Si	0.994	Tet Si	1.973	1.981	Tet Si	7.948
Fe	0.353	Al	0.027	0.019	Al	0.052
Mn	0.004	Σ	2.000	2.000	Σ	8.000
Mg	1.656	Oct Al	0.018	0.014	Oct Al	0.800
Σ	3.007	Ti	0	0	M1-3Ti	0
		Fe^{+3}	0.009	0	Fe^{+3}	0
		Cr	0	0.015	Cr	0
		Mg	1.622	0.931	Mg	5.350
		Fe^{+2}	0.314	0.091	Fe^{+2}	1.347
		Mn	0.005	0	Mn	0.043
		Ca	0.032	0.944	Σ	6.820
		Na	0	0	XM1-3	1.820
		K	0	0	M4 Ca	0.166
		Σ	2.000	1.995	Na	0
					Σ	1.986
					A Na	0
					K	0
					Σ	0
					OH	2
$\frac{Mg}{Mg+Fe^{+2}}$	0.82		0.84	0.91		0.80

Amphibole and pyroxene formulae calculated by the method developed by Papike *et al.* (1974) for maximum Fe^{+3}. Ideal H_2O assumed and analyses recalculated to 100.

Table 1. (cont.)

Analysis No.	5 Actinolite	6 Hornblende		7 Biotite		8 Spinel in Olivine	9 Spinel outside Olivine
SiO_2	56.31	43.70		39.38		0	0
TiO_2	0	1.60		1.74		1.01	0
Al_2O_3	2.35	12.34		15.84		20.77	64.83
Cr_2O_3	0.66	0.43		0.43		37.66	0
Fe_2O_3	0.47	8.37		0		6.55	0.83
FeO	3.56	0		6.29		28.55	19.92
MnO	0	0		0		0.51	0
MgO	21.81	17.05		22.48		4.74	14.24
CaO	12.65	11.95		0		0	0
Na_2O	0	1.50		0		0.20	0.16
K_2O	0	0.93		9.61		0	0
H_2O	2.18	2.11		4.22		0	0
Tet Si	7.749	6.209	Tet Si	5.597	Si	0	0
Al	0.251	1.791	Al	2.403	Al	0.780	1.984
Σ	8.000	8.000	Σ	8.000	Cr^{+3}	0.948	0
Oct Al	0.130	0.277	Oct Al	0.251	Fe^{+3}	0.235	0.024
M1-3Ti	0	0.171	Ti	0.185	Ti	0.024	0
Fe^{+3}	0.049	0.895	Fe^{+2}	0.748	Σ	1.988	2.008
Cr	0.072	0.049	Cr	0.048	Mg	0.225	0.551
Mg	4.473	3.610	Mn	0	Fe^{+2}	0.761	0.432
Fe^{+2}	0.409	0	Mg	4.762	Mn	0.014	0
Mn	0	0	Σ	5.994	Ca	0	0
Σ	5.134	5.003	Ca	0	Na	0.012	0.008
XM1-3	0.134	0.003	Na	0	K	0	0
M4 Ca	1.866	1.819	K	1.743	Σ	1.012	0.992
Na	0	0.177	Σ	1.743			
Σ	2.000	2.000	OH	4			
A Na	0	0.236					
K	0	0.169					
Σ	0	0.405					
OH	2	2					
$\frac{Mg}{Mg+Fe^{+2}}$	0.92	1.00		0.86		0.23	0.56

Table 2. REPRESENTATIVE ANALYSES FROM THE HOGANS ROAD DIORITE: 17,19,12, 11 FROM MSH19; 18 FROM MSH20; 10,13,20, 16 FROM MSH23; 14 FROM MSH43; 15 FROM MSH46.

Analysis No.	10	11	12	13		14	15
	Plagioclase					Clinopyroxene	
	rim		core				
SiO_2	57.89	55.56	49.48	45.41		52.68	53.42
TiO_2	0	0	0	0		0	0
Al_2O_3	26.86	28.6	32.28	35.00		2.31	0.60
Cr_2O_3	0	0	0	0		0.83	0.29
Fe_2O_3	0	0	0	0		0.33	0
FeO	0	0	0	0		4.40	7.38
MnO	0	0	0	0		0	0.28
MgO	0	0	0	0		16.04	14.02
CaO	8.65	10.17	15.60	18.79		23.42	24.01
Na_2O	6.61	5.25	2.64	0.80		0	0
K_2O	0	0.41	0	0		0	0
H_2O	0	0	0	0		0	0
Si	10.352	9.991	9.032	8.369	Tet Si	1.934	1.987
Al	5.662	6.063	6.946	7.606	Al	0.066	0.013
Ca	1.657	1.960	3.051	3.710	Σ	2.000	2.000
Na	2.291	1.830	0.933	0.287	Oct Al	0.033	0.014
K	0	0.095	0	0	Ti	0	0
Σ	19.962	19.939	19.962	19.972	Fe^{+3}	0.009	0
An	41.97	50.48	76.62	92.78	Cr	0.024	0.009
Ab	58.03	47.12	23.38	7.22	Mg	0.878	0.777
Or	0	2.40	0	0	Fe^{+2}	0.135	0.229
					Mn	0	0.009
					Ca	0.921	0.957
					Na	0	0
					K	0	0
					Σ	2.000	1.995
					$\frac{Mg}{Mg+Fe^{+2}}$	0.87	0.77

Table 2. (cont.)

Analysis No.	16 Actinolite	17 Hornblende		18 Biotite	19 Biotite		20 Prehnite
SiO_2	54.00	45.51		36.71	39.25		43.56
TiO_2	0.30	1.76		3.42	3.35		0.36
Al_2O_3	2.76	11.61		16.08	15.75		23.64
Cr_2O_3	0.55	0.35		0	0		0.28
Fe_2O_3	1.73	6.31		0	0		0.99
FeO	8.55	4.99		19.41	11.46		0
MnO	0.28	0		0	0		0
MgO	17.50	14.23		11.75	17.36		0
CaO	12.00	11.50		0	0		26.81
Na_2O	0.21	1.15		0	0		0
K_2O	0	0.50		8.63	8.67		0
H_2O	2.12	2.10		3.99	4.15		4.35
Tet Si	7.644	6.506	Tet Si	5.522	5.667	Si	6.002
Al	0.356	1.494	Al	2.478	2.333	Al	0
Σ	8.000	8.000	Σ	8.000	8.000	Σ	6.002
Oct Al	0.105	0.463	Oct Al	0.374	0.348	Al	3.841
M1-3 Ti	0.032	0.190	Ti	0.387	0.364	Fe^{+3}	0.103
Fe^{+3}	0.184	0.679	Fe^{+2}	2.442	1.383	Mg	0
Cr	0.061	0.039	Cr	0	0	Ti	0.038
Mg	3.691	3.031	Mn	0	0	Cr	0.030
Fe^{+2}	1.012	0.596	Mg	2.633	3.735	Σ	4.010
Mn	0.034	0	Σ	5.836	5.830	Ca	3.939
Σ	5.119	4.998	Ca	0	0	Na	0
XM1-3	0.119	0	Na	0	0	K	0
M4 Ca	1.820	1.762	K	1.657	1.597	Σ	3.959
Na	0.059	0.238	Σ	1.657	1.597	OH	4
Σ	1.879	2.000	OH	4	4		
A Na	0	0.081					
K	0	0.090					
Σ	0	0.171					
OH	2	2					
$\frac{Mg}{Mg+Fe^{+2}}$	0.76	0.70		0.52	0.73		

Table 3. REPRESENTATIVE ANALYSES FROM THE GARDENS GRANODIORITES: 22, 24, 26, 29, 30 FROM BT3/58; 21, 23, 25 FROM MBT258; 27 FROM MBT256; 28, 31 FROM BT3/60.

Analysis No.	21	22	23	24	25	26	27
	Clinopyroxene		Actinolite	Hornblende	Plagioclase core		Ilmenite
SiO_2	53.21	52.55	55.02	50.12	51.22	48.26	0.32
TiO_2	0.22	0	0	0.50	0	0	53.69
Al_2O_3	2.87	0.52	0.95	5.35	30.45	33.17	0.25
Cr_2O_3	1.14	0	0	0	0	0	0
Fe_2O_3	0	0	1.19	3.88	0	0	0
FeO	6.33	12.29	10.64	12.36	0	0	40.62
MnO	0	0.82	0.33	0.47	0	0	5.12
MgO	17.00	11.50	17.44	12.50	0	0	0
CaO	18.94	22.31	12.02	11.70	14.55	16.46	0
Na_2O	0.29	0	0.32	0.67	3.50	2.11	0
K_2O	0	0	0	0.38	0.28	0	0
H_2O	0	0	2.10	2.05	0	0	0

Clinopyroxene		21	22
Tet	Si	1.942	1.995
	Al	0.058	0.005
	Σ	2.000	2.000
Oct	Al	0.066	0.018
	Ti	0.006	0
	Fe^{+3}	0	0
	Cr	0.033	0
	Mg	0.925	0.651
	Fe^{+2}	0.193	0.390
	Mn	0	0.027
	Ca	0.741	0.908
	Na	0.021	
	K	0	
	Σ	1.984	
$\frac{Mg}{Mg+Fe^{+2}}$		0.83	0.63

Amphibole		23	24
Tet	Si	7.839	7.313
	Al	0.159	0.687
	Σ	7.998	8.000
Oct	Al	0	0.233
M1-3	Ti	0	0.055
	Fe^{+3}	0.127	0.426
	Cr	0	0
	Mg	3.703	2.717
	Fe^{+2}	1.267	1.508
	Mn	0.039	0.058
	Σ	5.137	4.997
XM1-3		0.137	0
M4	Ca	1.835	1.828
	Na	0.028	0.172
	Σ	2.000	2.000
A	Na	0.059	0.018
	K	0	0.072
	Σ	0.059	0.090
	OH	2	2
$\frac{Mg}{Mg+Fe^{+2}}$		0.75	0.58

Plagioclase	25	26
Si	9.344	8.832
Al	6.548	7.156
Ca	2.844	3.228
Na	1.236	0.748
K	0.068	0
Σ	20.040	19.964
An	68.56	81.19
Ab	29.80	18.81
Or	1.64	0

Ilmenite	27
Si	0.016
Ti	2.016
Al	0.015
Fe^{+2}	1.696
Mn	0.216
Σ	3.960

Table 3. (cont.)

Analysis No.	28	29		30		31
	Plagioclase rim			Biotite		Prehnite
SiO_2	59.16	55.68		37.02		42.72
TiO_2	0	0		3.66		1.25
Al_2O_3	25.98	28.14		14.89		19.88
Cr_2O_3	0	0		0		0.28
Fe_2O_3	0	0		0		5.24
FeO	0	0		20.46		0
MnO	0	0		0		0
MgO	0	0		10.83		0
CaO	7.89	10.77		0		26.35
Na_2O	6.97	5.41		0		0
K_2O	0	0		9.19		0
H_2O	0	0		3.95		4.28
Si	10.549	10.016	Tet Si	5.618	Si	5.988
Al	5.460	5.966	Al	2.382	Al	0.012
Ca	1.508	2.076	Σ	8.000	Σ	6.000
Na	2.410	1.886	Oct Al	0.281	Al	3.274
K	0	0	Ti	0.418	Fe^{+3}	0.552
Σ	19.927	19.944	Fe	2.596	Mg	0
An	38.49	52.40	Mn	0	Ti	0.132
Ab	61.51	47.60	Mg	2.448	Cr	0.031
Or	0	0	Σ	5.743	Σ	3.989
			Ca	0	Ca	3.957
			Na	0	Na	0
			K	1.779	K	0
			Σ	1.779	Σ	3.957
			OH	4	OH	4
			$\frac{Mg}{Mg+Fe^{+2}}$	0.49		

Table 4. REPRESENTATIVE ANALYSES FROM THE PYENGANA GRANODIORITES: 32, 33 FROM MAL1; 36 FROM MAL3; 34, 35 FROM MAL4.

Analysis No.	32	33		34		35	36
	Hornblende			Biotite		Plagioclase	
SiO_2	47.52	45.01		38.09		62.19	54.49
TiO_2	0.37	1.48		2.33		0	0
Al_2O_3	6.68	9.00		15.10		23.10	26.99
Cr_2O_3	0	0		0		0	
Fe_2O_3	3.60	6.48		0		0	
FeO	12.97	9.80		18.92		0	
MnO	0	0		0		0	
MgO	12.69	12.49		12.26		0	
CaO	11.90	11.42		0		10.77	13.26
Na_2O	1.69	1.46		0		5.23	5.05
K_2O	0.54	0.81		9.31		0	0.21
H_2O	2.03	2.04		3.99		0	0
Tet Si	7.006	6.615	Tet Si	5.723	Si	11.047	9.912
Al	0.994	1.385	Al	2.277	Al	4.836	5.784
Σ	8.000	8.000	Σ	8.000	Ca	1.235	2.584
Oct Al	0.166	0.174	Oct Al	0.397	Na	2.831	1.784
M1-3 Ti	0.042	0.164	Ti	0.264	K	0	0.048
Fe^{+3}	0.399	0.717	Cr	0	Σ	19.949	20.112
Cr	0	0	Fe^{+2}	2.377	An	30.37	58.51
Mg	2.789	2.736	Mn	0	Ab	69.63	40.40
Fe^{+2}	1.599	1.205	Mg	2.745	Or	0	1.09
Mn	0	0	Σ	5.783			
Σ	4.995	4.995	Ca	0			
XM1-3	0	0	Na	0			
M4 Ca	1.880	1.799	K	1.795			
Na	0.120	0.201	Σ	1.785			
Σ	2.000	2.000	OH	4			
A Na	0.364	0.215					
K	0.101	0.152					
Σ	0.465	0.367					
OH	2	2					
$\frac{Mg}{Mg+Fe^{+2}}$	0.63	0.69		0.55			

Table 5. REPRESENTATIVE ANALYSES FROM DOLERITE DYKE MBT74

Analysis No.	42	43		44	45		46
	Clinopyroxene			Plagioclase			Ilmenite
SiO_2	48.23	48.91		61.63	51.71		0
TiO_2	2.09	1.73		0	0		50.35
Al_2O_3	4.70	4.95		24.20	30.32		0
Cr_2O_3	0	0.35		0	0		0
Fe_2O_3	3.94	0.45		0	0		0
FeO	7.37	9.38		0	0		46.10
MnO	0.28	0		0	0		2.95
MgO	13.28	13.56		0	0		0
CaO	19.37	20.67		5.45	13.59		0.60
Na_2O	0.74	0		8.12	3.43		0
K_2O	0	0		0.60	0.94		0
H_2O	0	0		0	0		0
Tet Si	1.808	1.831	Si	10.948	9.427	Ti	0.967
Al	0.192	0.169	Al	5.067	6.517	Fe	0.985
Σ	2.000	2.000	Ca	1.036	2.655	Mn	0.064
Oct Al	0.016	0.049	Na	2.798	1.211	Ca	0.016
Ti	0.059	0.049	K	0.136	0.220	Σ	2.032
Fe^{+3}	0.111	0.013	Σ	19.985	20.030		
Cr	0	0.010	An	26.09	64.98		
Mg	0.742	0.756	Ab	70.46	29.64		
Fe^{+2}	0.231	0.294	Or	3.45	5.37		
Mn	0.009	0					
Ca	0.778	0.829					
Na	0.054	0					
K	0	0					
Σ	2	2					
$\frac{Mg}{Mg+Fe^{+2}}$	0.76	0.72					

Table 6. REPRESENTATIVE ANALYSES FROM DOLERITE DYKE 136.

Analysis No.	36	37		38	39		40		41
	Hornblende			Plagioclase			Biotite		Ilmenite
SiO_2	47.57	49.18		49.73	55.96		37.16		0
TiO_2	0.51	0.58		0	0		1.73		52.26
Al_2O_3	8.33	6.45		32.62	28.43		16.34		0
Cr_2O_3	0.25	0.23		0	0		0.12		0
Fe_2O_3	10.21	6.70		0	0		0		0
FeO	5.06	10.89		0	0		16.91		46.09
MnO	0	0.27		0	0		0		1.49
MgO	13.88	14.88		0	0		14.93		0
CaO	10.66	7.63		15.24	10.05		0.48		0.17
Na_2O	1.26	0.85		2.41	5.35		0		0
K_2O	0.18	0.24		0	0.20		8.29		0
H_2O	2.09	2.07		0	0		4.04		0
Tet Si	6.833	7.107	Si	9.051	10.044	Tet Si	5.519	Ti	0.994
Al	1.167	0.893	Al	7.000	6.016	Al	2.481	Fe	0.975
Σ	8.000	8.000	Ca	2.972	1.933	Σ	8.000	Mn	0.032
Oct Al	0.243	0.206	Na	0.852	1.863	Oct Al	0.378	Ca	0.005
M1-3									
Ti	0.055	0.063	K	0	0.046	Ti	0.193	Σ	2.006
Fe^{+3}	1.104	0.729	Σ	19.975	19.902	Fe^{+2}	2.100		
Cr	0.028	0.027	An	77.72	50.31	Cr	0.014		
Mg	2.970	3.204	Ab	22.28	48.49	Mn	0		
Fe^{+2}	0.608	1.316	Or	0	1.20	Mg	3.304		
Mn	0	0.034				Σ	5.989		
Σ	5.009	5.579				Ca	0.076		
XM1-3	0.009	0.579				Na	0		
M4 Ca	1.641	1.182				K	1.571		
Na	0.351	0.239				Σ	1.647		
Σ	2.000	2.000				OH	4		
A Na	0	0							
K	0.032	0.045							
Σ	0.032	0.045							
OH	2	2							
$\frac{Mg}{Mg+Fe^{+2}}$	0.83	0.71					0.61		

Table 7. $K_{D\ (Fe-Mg)}^{ol/l}$ *CALCULATED FOR ROCKS FROM THE HOGANS ROAD DIORITE.*

K_D = (Fe/Mg) olivine/(Fe/Mg) liquid;

K_{D_1} calculated with Fe^{+2} as analysed;

K_{D_2} calculated with all the iron as Fe^{+2}.

Olivine composition used was analysis 1 in Table 1.

Rock number	K_{D1}	K_{D2}
MSH20	0.290	0.257
MSH23	0.499	0.449
MSH19	0.658	0.625
MSH22	1.175	0.984

Table 8. RESULTS OF MIXING CALCULATIONS. R STANDS FOR RESIDUAL.

Numbers in brackets after mineral names refer to the analyses numbers in Tables 1-6.

(A) MSH20 + olivine(1) + orthopyroxene(2) + clinopyroxene(3) = MSH22
0.366 0.277 0.142 0.215 1
ΣR^2 = 4.76

(B) olivine(1) + orthopyroxene(2) + clinopyroxene(3) + plagioclase(12)
0.244 0.291 0.212 0.211
+ H_2O + K_2O = MSH22
0.022 0.011 1
ΣR^2 = 1.49

(C) MAL5 + hornblende(33) + plagioclase(36) + biotite(34) + apatite
0.819 0.066 0.062 0.048 0.003
+ sphene = MAL1
0.002 1
ΣR^2 = 0.124

(D) MBT255 + hornblende(24) + plagioclase(26) + biotite(30)
0.685 0.172 0.121 0.017
+ ilmenite(27) = BT3/58
0.005 1
ΣR^2 = 1.216

(E) BT3/58 + hornblende(37) + plagioclase(38) + biotite(40)
0.026 0.433 0.416 0.096
+ ilmenite(41) + apatite = 136
0.021 0.007 1
ΣR^2 = 1.691

APPENDIX 1

Whole rock analyses for the Pyengana granodiorite, Gardens granodiorite and the Hogans Road diorite.

	MAL1	MBT259	MAL2	MAL3	MAL4	MBT260	MAL5	MAL7
SiO_2	64.52	65.01	65.23	65.30	65.59	65.74	68.67	69.71
TiO_2	0.50	0.51	0.49	0.50	0.48	0.46	0.27	0.40
Al_2O_3	14.92	14.93	15.21	15.03	15.15	14.60	14.50	14.47
Fe_2O_3	1.51	1.05	1.38	1.22	1.54	1.16	0.92	0.90
FeO	3.15	3.46	3.08	3.23	3.00	3.08	2.09	2.26
MnO	0.07	0.08	0.07	0.08	0.08	0.08	0.06	0.06
MgO	2.58	2.67	2.55	2.63	2.53	2.45	1.55	1.29
CaO	4.38	4.24	4.32	4.28	4.35	3.89	3.11	3.04
Na_2O	2.38	2.35	2.36	2.20	2.43	2.50	2.62	1.90
K_2O	3.59	3.47	3.48	3.36	3.30	3.59	3.68	3.51
P_2O_5	0.21	0.22	0.21	0.20	0.20	0.18	0.10	0.10
CO_2	0.15	0.11	0.06	0.14	0.12	0.08	0.09	0.15
H_2O^+	1.15	1.41	1.21	1.54	1.35	1.47	1.23	0.95
H_2O^-	0.40	0.29	0.20	0.28	0.12	0.14	0.10	0.31
Total	99.51	99.80	99.85	99.99	100.24	99.42	99.99	99.41
				ppm				
Sn	8	48	5	8	4	12	12	7
Th	23	20	22	21	27	22	30	15
Sr	360	350	420	400	410	330	330	160
U	7	7	11	9	7	11	10	6
Rb	185	200	180	180	185	210	200	165
Y	23	27	22	22	22	22	19	31
Zr	140	140	150	145	155	135	100	140
Nb	7	7	8	7	9	7	8	7
Pb	21	18	22	21	21	22	30	26
As	<10	<10	11	<10	<10	<10	<10	11
Ga	16	15	16	15	16	14	15	16
Zn	61	75	56	57	58	69	48	56
Cu	17	39	14	24	27	31	18	23
Ni	18	19	16	16	15	16	10	6
Sc	14	14	14	13	15	13	10	12
V	105	105	95	97	97	91	56	58
Cr	46	46	38	37	36	140	18	17
Co	13	12	11	11	10	11	7	6
Ba	660	610	650	630	670	590	570	540

Appendix 1 (continued)

	BT3/58	MBT258	MBT253	MBT257	BT3/60	BT3/59	BT3/61	MBT255
SiO_2	62.36	64.37	64.57	65.00	69.08	69.15	69.27	69.68
TiO_2	0.63	0.55	0.64	0.53	0.41	0.39	0.40	0.29
Al_2O_3	14.94	15.20	15.46	15.17	14.44	14.56	14.55	14.25
Fe_2O_3	0.98	1.25	1.08	1.21	0.88	0.84	0.77	0.70
FeO	4.45	3.53	3.61	3.46	2.62	2.62	2.62	2.39
MnO	0.09	0.07	0.07	0.07	0.06	0.06	0.06	0.06
MgO	3.33	2.95	2.53	2.70	1.67	1.67	1.61	1.51
CaO	5.65	4.85	4.69	4.76	3.44	3.44	3.55	2.77
Na_2O	2.03	2.43	2.56	2.66	2.86	2.51	2.77	2.92
K_2O	2.17	2.91	2.68	2.98	3.22	3.58	3.19	3.71
P_2O_5	0.17	0.14	0.17	0.13	0.10	0.11	0.10	0.12
CO_2	0.15	0.10	0.17	0.11	0.10	0.10	0.10	0.11
H_2O^+	1.99	1.21	1.45	1.29	1.16	1.18	1.56	1.04
H_2O^-	0.21	0.15	0.14	0	0.13	0.02	0	0.17
Total	99.15	99.71	99.82	100.07	100.17	100.23	100.55	99.72
				ppm				
Sn	10	7	6	5	15	6	18	7
Th	11	17	17	23	23	18	19	16
Sr	320	310	330	310	260	290	270	180
U	4	5	7	7	6	5	7	13
Rb	115	130	115	145	160	160	150	210
Y	24	18	20	17	22	20	21	16
Zr	155	130	170	140	135	125	140	93
Nb	4	6	7	5	6	6	6	7
Pb	13	21	17	22	30	37	29	37
As	11	<10	<10	<10	<10	<10	<10	15
Ga	17	15	16	16	15	15	15	13
Zn	73	62	61	64	59	67	56	63
Cu	13	16	17	15	11	12	11	16
Ni	12	17	10	15	7	6	7	6
Sc	20	13	13	14	11	13	10	<9
V	125	105	93	97	63	66	62	52
Cr	70	56	38	40	26	25	22	31
Co	14	14	12	14	9	7	8	8
Ba	510	510	610	590	560	820	590	380

Appendix 1 (continued)

	MBT256	MSH22	MSH20	MSH19	MSH23
SiO_2	72.54	47.20	48.80	51.87	53.97
TiO_2	0.26	0.31	0.96	0.47	0.54
Al_2O_3	13.67	6.88	17.63	10.77	12.23
Fe_2O_3	0.54	1.57	1.26	0.49	0.93
FeO	1.71	7.29	8.80	8.54	7.63
MnO	0.03	0.15	0.20	0.17	0.15
MgO	0.58	22.58	6.73	14.81	10.04
CaO	1.79	8.52	9.97	8.33	9.05
Na_2O	2.78	0.55	1.31	0.66	0.93
K_2O	4.86	0.92	1.53	1.45	1.53
P_2O_5	0.05	0.21	0.20	0.16	0.15
CO_2	0.10	0.15	0.05	0.11	0.08
H_2O^+	0.76	2.03	2.12	2.23	2.02
H_2O^-	0.11	0.09	0.10	0.09	0.09
Total	99.78	98.45	99.66	100.15	99.34
			ppm		
Sn	5	<3	5	<3	<3
Th	26	9	10	10	8
Sr	165	370	420	300	170
U	7	2	2	2	4
Rb	240	30	61	59	74
Y	30	11	18	13	13
Zr	185	53	78	52	74
Nb	9	<3	<3	<3	<3
Pb	41	<4	4	<7	<4
As	<10	<10	18	62	<10
Ga	14	6	17	13	13
Zn	26	73	105	90	91
Cu	11	29	15	15	19
Ni	4	280	12	120	18
Sc	<9	34	40	33	37
V	28	145	290	185	220
Cr	<5	2100	64	1050	390
Co	<6	64	34	48	33
Ba	700	430	400	420	200

APPENDIX 2

Whole rock analyses for dolerite dykes from the Blue Tier and Ringarooma map sheets

	MBT72	MBT74	MBT77	BT22	BT28	BT30	BT31	30
SiO_2	48.7	46.0	57.8	47.6	48.0	47.9	48.6	48.5
TiO_2	1.8	2.2	1.9	2.0	1.7	3.1	2.1	2.8
Al_2O_3	15.5	14.9	15.4	15.0	15.2	12.9	15.0	14.4
Fe_2O_3	2.9	2.5	0.51	3.0	3.7	2.2	1.5	1.7
FeO	8.3	9.7	7.1	8.7	7.8	11.9	9.3	11.8
MnO	0.21	0.23	0.14	0.2	0.19	0.26	0.19	0.23
MgO	6.3	6.7	3.1	7.3	7.4	6.1	6.7	5.1
CaO	9.0	9.3	6.5	9.1	10.4	8.4	9.2	8.5
Na_2O	3.0	3.2	3.0	2.8	2.5	2.7	2.2	2.4
K_2O	0.63	0.55	1.4	0.65	0.14	0.47	0.65	1.2
P_2O_5	0.45	0.23	0.64	0.30	0.24	0.70	0.47	0.39
CO_2	0.13	0.34	0.15	-	-	-	-	-
H_2O^+	2.5	3.1	1.8	3.5	2.8	3.2	3.0	2.0
H_2O^-	-	-	-	0.39	0.30	0.28	0.36	-
Total	99.42	98.95	99.44	100.54	100.37	100.11	99.27	99.02
				ppm				
Li	15	25	35	32	36	20	38	40
Sn	-	-	-	5	<5	<5	<5	-
Sr	310	260	550	260	227	282	244	265
Rb	11	36	49	39	3	23	31	155
Y	35	33	32	37	41	50	41	60
Zr	160	130	290	132	122	363	291	215
Nb	15	4	23	<4	8	16	12	-
Zn	140	120	100	121	103	172	143	235
Ni	51	67	29	50	61	33	50	58
V	300	340	86	-	-	-	-	-
Co	47	49	16	39	48	43	37	-
Ba	230	110	500	-	-	-	-	-

Appendix 2 (continued)

	136	146	65	66
SiO_2	47.1	48.4	49.8	48.8
TiO_2	1.5	1.2	1.4	3.1
Al_2O_3	18.2	16.9	16.1	14.1
Fe_2O_3	1.5	2.0	1.8	1.8
FeO	8.4	7.3	8.2	12.1
MnO	0.19	0.16	0.20	0.24
MgO	8.1	8.1	7.6	5.4
CaO	9.9	10.7	10.1	9.0
Na_2O	2.5	2.5	2.6	2.7
K_2O	0.53	0.29	0.28	0.65
P_2O_5	0.32	0.15	0.22	0.63
CO_2	-	-	-	-
H_2O^+	1.6	2.0	1.8	1.5
H_2O^-	-	-	-	-
Total	99.84	99.70	100.10	100.02
		ppm		
Li	20	30	25	40
Sn	-	-	-	-
Sr	167	160	249	286
Rb	27	27	27	40
Y	30	59	32	55
Zr	215	26	90	264
Nb	-	-	6	15
Zn	129	104	165	214
Ni	97	48	44	53
V	-	-	-	-
Co	-	-	39	41
Ba	-	-	-	-

APPENDIX 3

Distribution coefficients used to construct fractionation vectors

	olivine	plagioclase	clinopyroxene	orthopyroxene	hornblende	biotite
Rb	0.0113	0.071	0.0056	0.022	0.01	3.26
Zr	0.01	0.01	0.1	0.03	4	2
Ti	0.02	0.04	0.3	0.1	7	2.5
Y	0.01	0.03	0.5	0.2	6	0.03

Data from Pearce and Norry (1979), Perfit *et al.* (1980) and Higgins *et al.* (1983).